Thermochimica Acta 499 (2010) 1–7

Contents lists available at ScienceDirect

Thermochimica Acta

journal homepage: www.elsevier.com/locate/tca

Using heat conduction microcalorimetry to study thermal aggregation kinetics of proteins

Donghua (Alan) Zhu[a], William R. Porter[a], Michelle A. Long[b], Wolfgang Fraunhofer[c], Kenneth M. Gleason[a], Yi Gao[a,*]

[a] Pharmaceutics, Abbott Laboratories, 100 Abbott Park Road, Abbott Park, IL 60064-6120, United States
[b] Physical Characterization, Manufacturing Sciences and Technology, Abbott Laboratories, 1401 Sheridan Road, North Chicago, IL 60064, United States
[c] Pharmaceutics, Abbott Bioresearch Center, 100 Research Drive, Worcester, MA 01605, United States

ARTICLE INFO

Article history:
Received 24 March 2009
Received in revised form 4 August 2009
Accepted 16 October 2009
Available online 29 October 2009

Keywords:
Monoclonal antibody
Isothermal microcalorimetry
Micro-differential scanning calorimetry
Size exclusion chromatography

ABSTRACT

The thermally induced irreversible aggregation of a monoclonal antibody in different pH buffers was investigated using different techniques such as micro-differential scanning calorimetry (micro-DSC), size exclusion HPLC (SEC) and isothermal microcalorimetry. The kinetics of aggregation of the protein was analyzed in terms of a Lumry–Eyring model proceeding via a non-native conformational state. The rate constants and reaction enthalpies of unfolding and consequent aggregation were obtained by fitting the isothermal microcalorimetric and SEC data based on proposed aggregation mechanisms. The consistency of rate constants obtained via isothermal microcalorimetry and SEC indicates it is possible to deconvolute the observed microcalorimetry power–time data obtained from thermally induced protein aggregation.

1. Introduction

Formulation of proteinaceous drugs poses unique challenges due to the complex physicochemical properties intrinsic to these macromolecules [1]. For some protein pharmaceuticals, thermally induced protein aggregation is the dominant degradation route that could eliminate or reduce their activities [2]. Protein unfolding (denaturation) is generally accepted to be the rate-determining step in protein aggregation, followed by the quick association of unfolded protein molecules to form the actual aggregates [3]. Some proteins such as human interferon-γ have been reported to aggregate irreversibly when exposed to low pH or elevated temperatures [4].

During the last two decades, a number of original papers and reviews have reported kinetic studies on unfolding and aggregation mechanisms of different proteins using several techniques including size exclusion high performance liquid chromatography (SEC), micro-differential scanning calorimetry (micro-DSC) and circular dichroism spectroscopy (CD) [5–7]. Because of the different signal detection principles of these techniques, often at least two different techniques must be employed to describe the mechanism completely. The resulting sample collection and instrumental calibration procedures are labor-intensive. Of these methods, only CD permits continuous monitoring as reaction time and temperature are varied.

Thermal activity monitor (TAM), the most frequently used isothermal microcalorimeter, is widely used for studying chemical reactions (e.g., degradation, drug-exicipient compatibility) and/or physical processes (e.g., relaxation, crystallization) of sample substances at a constant temperature [8–10]. Because of its high sensitivity, continuity of response over time and labor saving sample preparation characteristics, isothermal microcalorimetry is a useful tool for studying the mechanism of reacting systems. Beezer et al. introduced a method to deconvolute consecutive reaction schemes measured by isothermal microcalorimetry that overcomes the non-specific nature of the technique [8]. These instrumental and theoretical strengths allow us to choose a novel approach based on calorimetric methods to determine both kinetic parameters and reaction enthalpy associated with protein unfolding and consequent aggregation.

In this paper, we propose a method for the analysis of the kinetics of protein unfolding and aggregation at elevated temperatures using isothermal microcalorimetry and extend the method for stability screening of protein formulations. A monoclonal antibody (Abbott-X) was selected as a model protein. SEC and micro-DSC were used to describe and further confirm the reaction mechanism demonstrated by isothermal microcalorimetry.

* Corresponding author. Tel.: +1 847 937 9028; fax: +1 847 938 4434.
E-mail address: gao.yi@abbott.com (Y. Gao).

0040-6031/$ – see front matter © 2009 Elsevier B.V. All rights reserved.
doi:10.1016/j.tca.2009.10.012

2. Experimental

2.1. Materials

The purified human monoclonal antibody (Abbott-X) developed in Abbott Laboratories to potentially treat T cell-mediated autoimmune disease, sepsis and acute or chronic liver disease, was used in this study. This protein has a molecular weight of ~150 kD and a p*I* (isoelectric point) value of 8.2. All other materials and reagents were of analytical grade. The antibody was dissolved in buffers containing 10 mM citric acid and 10 mM phosphoric acid adjusted with sodium hydroxide to pH 3.4, 5.3, 6.1 or 7.4, respectively. Buffers commonly used in biologics formulation such as histidine- or Tris-based systems have high ionization enthalpies, which makes the buffer pH values susceptible to temperature changes. For this particular reason, the citrate/phosphate mixed buffer was chosen to maintain stable pH values over a broad temperature range for the thermal stability studies [11].

2.2. Thermostability studies

2.2.1. Micro-DSC

Heat flow was measured as a function of temperature of monoclonal antibody samples (7.8 and 29 mg/mL in citrate/phosphate mixed buffer, respectively) at scanning rates of 0.1–1 °C/min using a micro-differential scanning calorimeter (model Micro-DSC III, Setaram SAS, Caluire, France) in standard batch vessels. In order to improve the sensitivity but not to sacrifice the resolution, the combination of large sample mass (29 mg/mL, 0.1 mL) and slow heating rate was selected to characterize the thermal denaturation of Abbott-X. When in studying temperature dependence of the unfolding on the scanning rates, a smaller sample mass (7.8 mg/mL, 0.2 mL) was used. Indium standards were used for temperature and heat of fusion calibration. The performance of the micro-DSC was confirmed using naphthalene.

2.2.2. Size exclusion chromatography

Protein samples (29 mg/mL in citrate/phosphate mixed buffers at various pH values) were incubated for specified periods of time under controlled temperatures in hermetically sealed glass vials. Incubated samples were then quenched by 20-fold dilution with cold citrate/phosphate mixed buffer at the same pH value. SEC was performed on a Model 1100 HPLC System (Agilent Technologies, Palo Alto, CA) by injecting 20 μL diluted sample to a Superdex^{TM} 200 10/300 GL column with 50 mM Na_2HPO_4, 150 mM NaCl, pH 7.0 as the mobile phase at a flow rate of 0.5 mL/min. The column eluent was monitored at 214 nm. The aggregation of the protein-formation of dimmers and high order aggregates was described with reference to the gel filtration standard (Bio-Rad, Hercules, CA).

2.2.3. Thermal activity monitor

All studies employed a thermal activity monitor (TAM model 2277, Thermometric AB, Sweden) consisting of four calorimetric units (part # 2277-201) and standard amplifiers. Data collection and analysis were performed using DIGITAM for Windows version 4.1 software (Thermometric AB, Sweden). Each channel of the calorimeter was electrically calibrated with a precision of ±0.2% before starting a series of experiments at a predetermined temperature and during the course of the study. In order to obtain higher sensitivity, 4 mL stainless steel cylinders were used to contain the samples. The thermal activity was measured against a reference of protein-free buffer loaded into identical cylinders. Thermal activity of protein samples (29 mg/mL in citrate/phosphate mixed buffers at various pH values, $n = 3$) was monitored isothermally at 50, 55, 58 or 60 °C, respectively. Sample volumes were 350 μL at 50 °C, 350 μL or 200 μL at 55 °C; 150 μL at 58 °C and 100 μL at 60 °C. In general, the thermal signal is much stronger at higher temperatures since the reactions occur at higher rates. Since the reaction rates are independent of sample mass, in order to save the precious protein material, a small volume at higher experimental temperatures was used in the study. Due to the thermal disturbance induced during sample loading, the thermal signal from the first ~2 h was not included in the data analysis. The reproducibility of the thermal signal even with different sample mass was found to be acceptable with a standard deviation around 8% ($n = 3$), as exemplified by Abbott-X at pH 3.4 at 55 °C shown in Fig. 1.

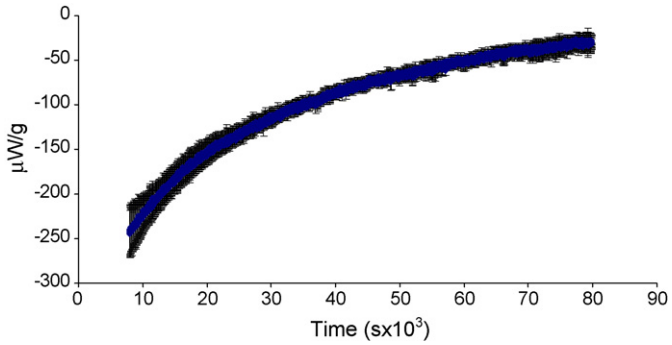

Fig. 1. Power–time plot for Abbott-X at pH 3.4 at 55 °C (blue line: average signal; black bar: standard deviation, $n = 3$). (For interpretation of the references to color in this figure legend, the reader is referred to the web version of the article.)

2.2.4. Data analysis

Differential kinetic models described below were fitted to the data using Scientist® software (Micromath Scientific Software Inc., St Louis, MO).

3. Results

3.1. Micro-DSC

Thermal denaturation of Abbott-X buffered at different pH values was studied by micro-DSC. Typical thermograms of the protein in the citrate/phosphate buffer, pH 6.1 and pH 3.4, with a scan rate 0.5 °C/min are shown in Fig. 2A and B, respectively. The curve for the protein at pH 6.1 shows two endothermic transitions, one at a denaturation temperature (T_m) at 70.5 °C with an apparent denaturation enthalpy (ΔH_{un}) of about 21.3 J/g, and a second T_m at 82.2 °C with an enthalpy about 1.41 J/g. The presence of two peaks for the protein at pH 6.1 indicates that at least two domains or two groups of domains exhibit denaturation under distinct conditions. However, at a more extreme pH value, pH 3.4, the thermogram of the protein contains only one endothermic peak characterized by a T_m of 66.5 °C and apparent ΔH_{un} of about 13.4 J/g. It can be inferred from these results that the structure of Abbott-X is highly influenced by the pH. Although more than one T_m were observed for Abbott-X under some pH conditions, the lower temperature T_m (first T_m) will be defined as the denaturation temperature because the protein will lose or have reduced activity after the disruption of the first domain or domain group. Under all of the tested conditions described above, the DSC thermograms were irreversible based on the observation that the Abbott-X formed gel-like mass (clearly denatured/aggregated) after the sample was cooled down to ambient temperature. A larger unfolding enthalpy may imply a greater degree of intermolecular interaction at pH 6.1 thus requiring greater energy to dissociate. However, given the unspecific nature of DSC and the irreversible DSC thermograms of Abbott-X (aggregation immediately upon unfolding), it is difficult to deconvolute the peak area to separate the unfolding enthalpy from aggregation enthalpy. Thus, it is reasonable to use the denaturation

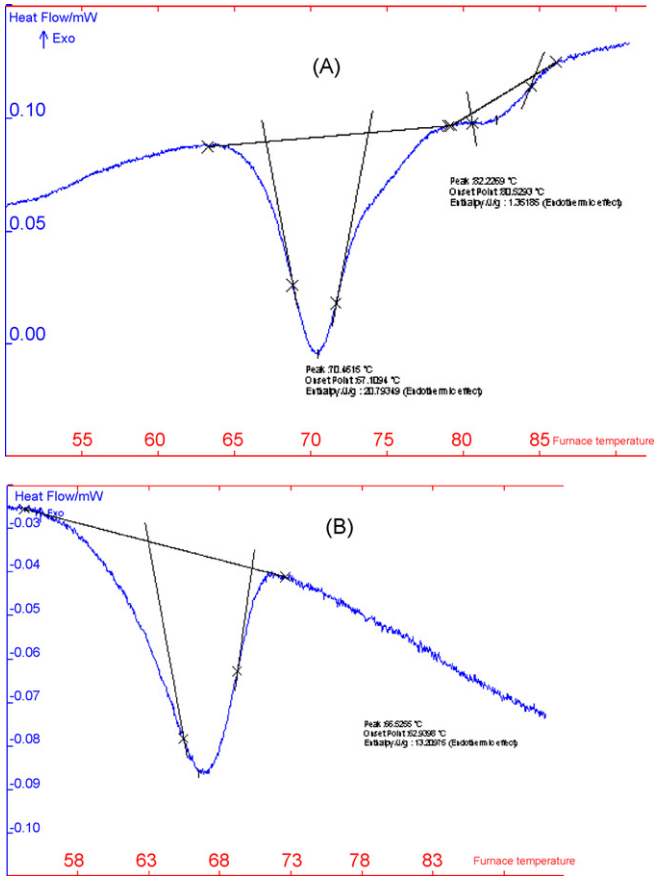

Fig. 2. Micro-DSC thermograms of the monoclonal antibody Abbott-X (29 mg/mL in citrate phosphate buffer) at pH 6.1 (A) and pH 3.4 (B).

temperatures (data shown in Table 1) to rank order the stability of Abbott-X in various formulations.

3.2. Size exclusion chromatography

The analysis by SEC demonstrates that aggregation is the major degradation pathway for Abbott-X in the thermally induced degradation. A typical SEC chromatogram as a function of time for the protein monomer solution at pH 3.4 and pH 6.1 at 55 °C is shown in Fig. 3A and B. The observed aggregation peak shifts in the chromatogram over time from right (longer retention time) to left (shorter retention time), indicating an increase in molecular weight. Based on the retention times of molecular weight standards, the Abbott-X aggregates grow from a non-native monomer to a dimer and eventually to a pentamer. Higher order aggregates were not able to be observed by SEC because of their low solubility in solution. It was observed visually that the initially clear and particulate-free samples became progressively hazy and finally formed gels. The aggregation kinetics of Abbott-X at pH 3.4, 55 °C was demonstrated in Fig. 4.

Table 1
T_m of the monoclonal antibody Abbott-X (7.8 mg/mL in citrate/phosphate buffer, $n = 3$) at different pH values measured at a heating rate of 1 °C/min.

pH	Ave. T_m (°C)
3.4	68.2 (±0.2)
5.3	71.8 (±0.4)
6.1	72.2 (±0.4)
7.4	71.4 (±0.2)

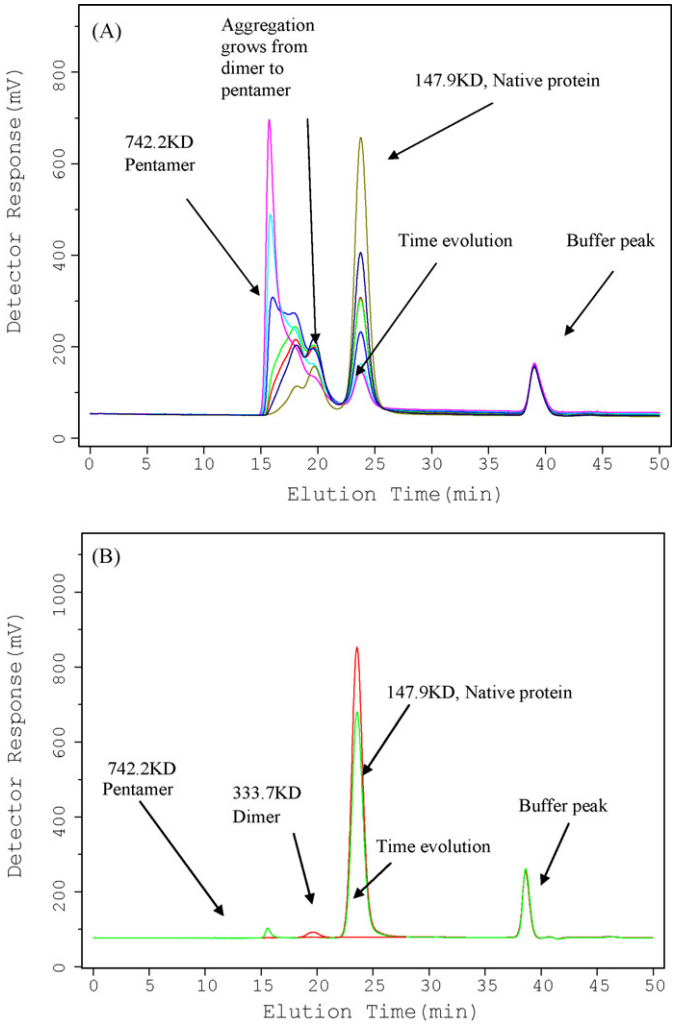

Fig. 3. (A) SEC-HPLC chromatograph showing the time evolution of aggregation from monomer to dimer and further to pentamer for the protein Abbott-X buffered at pH 3.4 (A) and pH 6.1 (B) at 55 °C.

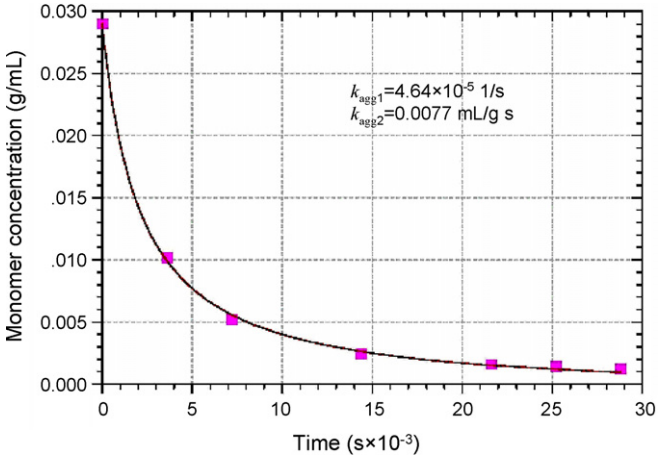

Fig. 4. Aggregation kinetic profile for the monoclonal antibody Abbott-X at pH 3.4 at 55 °C: squares: experimental data from SEC HPLC; solid black line: fitted line (data was fitted into Eq. (2), model selection criterion = 6.8).

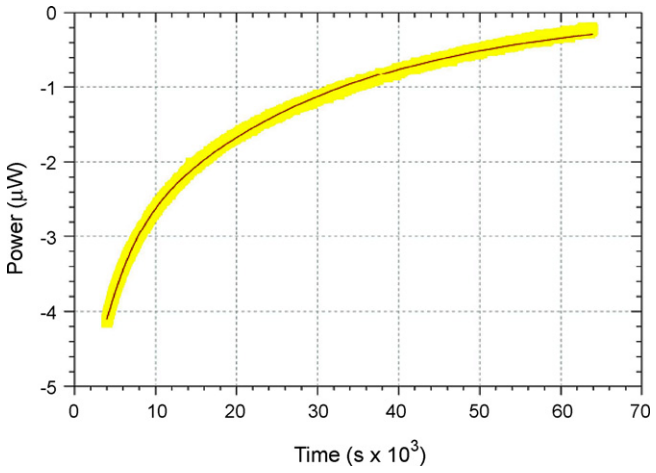

Fig. 5. Fitted power–time plot for Abbott-X at pH 3.4 at 55 °C using Eq. (8). Black thin line: fitted line; broad yellow line: experimental data from TAM (data was fitted into Eq. (8), model selection criterion = 6.7). (For interpretation of the references to color in this figure legend, the reader is referred to the web version of the article.)

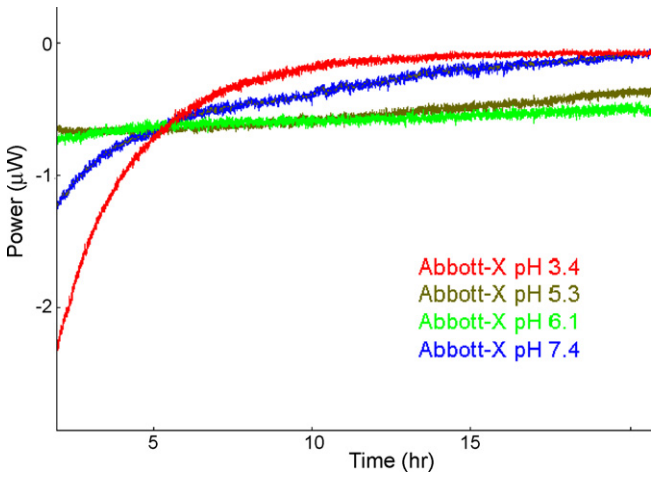

Fig. 6. Power–time curves of Abbott-X at different pHs at 60 °C. (For interpretation of the references to color in this figure legend, the reader is referred to the web version of the article.)

3.3. Thermal activity monitor

Monitoring thermal activity is a non-specific technique [10]. The measured signal represents the overall heat absorbed or liberated in the process. The rate equation to describe the process in terms of heat flow is [10]:

$$\frac{dq}{dt} = -V \sum \left(\Delta H_i \frac{dn_i}{dt} \right) \quad (1)$$

where dq/dt is the power signal (μW) and V is the volume of the sample (mL), ΔH_i is the enthalpy change for the process i (J/g) and dn_i/dt is the rate of process i (g/(mL s)).

In our study, the overall heat flow is the net contribution of two consecutive reactions, protein unfolding, which is endothermic, and aggregation, which is exothermic. One example of the power–time curves shown in Fig. 5 represents the thermal activity of Abbott-X at pH 3.4 and 55 °C (experimental data: broad yellow line). In general, this type of curves monotonically approaches to the base line (signal zero) from its initiate negative (endothermic) signal while the protein undergoes the process of unfolding and aggregation.

A comparison of the slopes of the power–time curves provides a straightforward way to estimate the stable pH range of protein formulations. In this case, we used the slopes of the power–time curves from $t_{4\,h}$ to $t_{5\,h}$ as shown in Fig. 6 to rank order the relative stability of Abbott-X at four different pHs. As shown in Fig. 6, the sample at pH 3.4 clearly displays the sharpest slope, indicating the worst stability among the four pH conditions. The second worst is evidently pH 7.4. For samples at pH 5.3 and 6.1, due to slower reactions (unfolding and aggregation), the resulting thermal change is too small to be differentiated. Therefore, the optimal pH range for storing the monoclonal antibody is between pH 5 and pH 6. This is consistent with the stability rank order based on T_m from micro-DSC (data shown in Table 1) as well as by the pH stability profile previously obtained by HPLC (shown in Fig. 7). These results demonstrate the utility of using TAM as a screen tool to narrow down the formulation spaces or conditions. A follow-up study using more accurate but more time consuming methods (such as HPLC) can then be conducted to pinpoint the most optimal formulation conditions. By doing so, significant savings in time and cost can be achieved since the second study can be done in a narrower range of conditions.

4. Discussion

4.1. The relationship between T_m and the stability of Abbott-X

The stability of the protein is mainly measured by two types of techniques: optical and thermal techniques. The first ones include UV spectrophotometry, fluorescence and circular dichroism. These methods are sensitive to protein conformation and thus require less material than the latter ones, thermal techniques such as differential scanning calorimetry which provides the thermodynamics of unfolding of proteins. Empirical stability parameters such as denaturation temperature (T_m) can easily be determined using DSC. Given a higher sensitivity offered by micro-DSC, the same result can be obtained from samples at 1/10th the concentration previously required using conventional DSC. The T_m is directly related to protein stability with a higher T_m indicating greater stability; therefore the T_m measurement can aid in early formulation development where optimal stability is desired [9]. For example, the optimal formulation pH range can be determined by comparing the values of T_m under different pH conditions. The comparison of T_m of Abbott-X as a function of pH is shown in Table 1. In this case, Abbott-X exhibits maximum stability at about pH 6.1 among the four pHs studied, which is consistent with the results obtained in a previous study where a gold standard method (HPLC) was used, as shown in Fig. 7. It also agrees well with the comparison of activation energy for the denaturation (unfolding) of Abbott-X at different pH val-

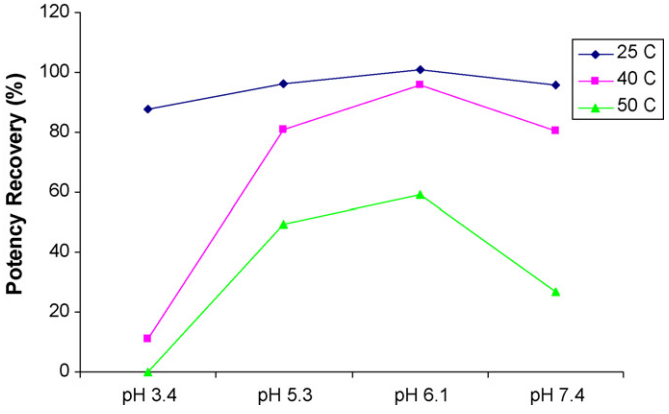

Fig. 7. Potency recovery of Abbott-X after 7 days' incubation under various conditions.

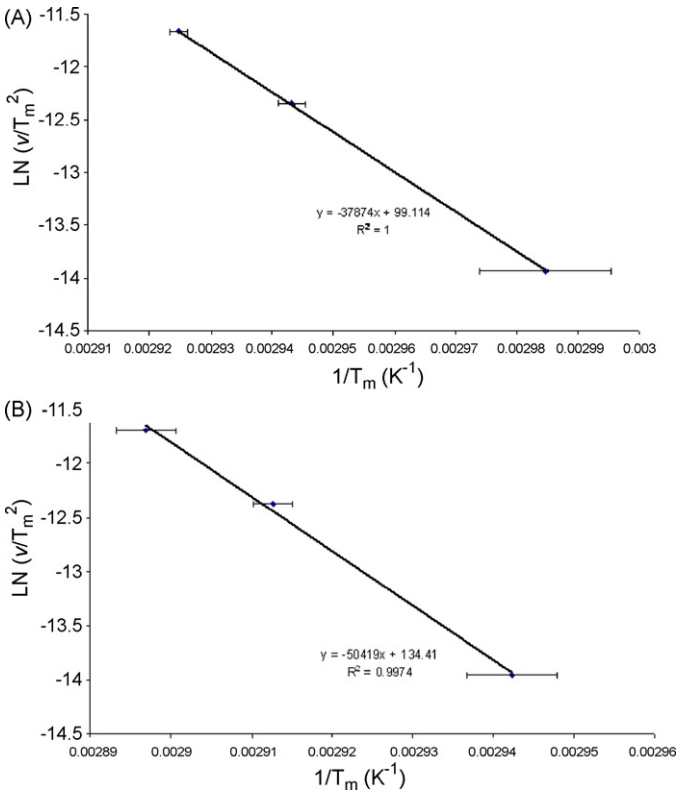

Fig. 8. Plots of $\ln(\nu/T_m^2)$ versus $1/T_m$: Abbott-X protein buffered at pH 3.4 (A) and pH 6.1 (B) ($n = 3$).

ues. In general, activation energy for the denaturation of a protein can be calculated based on the previously established model [12] as described below. Briefly, T_m varies with heating rate (ν, °C/min) according to:

$$\ln\left(\frac{\nu}{T_m^2}\right) = \ln\left(\frac{AR}{E_a}\right) - \frac{E_a}{RT_m} \quad (2)$$

In Eq. (2), A (min^{-1}) is the Arrhenius frequency factor, E_a (kJ/mol) is the activation energy of unfolding, and R is the gas constant. A plot of $\ln(\nu/T_m^2)$ versus $1/T_m$ should result in a linear line with a slope of $-E_a/R$, from which E_a can be calculated. Such plots were constructed for Abbott-X at pH 6.1 and pH 3.4 and shown in Fig. 8A and B, respectively. The irreversible DSC thermograms as well as their scan-rate dependence can be explained by assuming that the thermal denaturation of Abbott-X follows the kinetic scheme of N to D, a pseudo-first-order reaction, where E_a is an apparent activation energy, as given by the Arrhenius equation. The E_a values are calculated to be 419 and 315 kJ/mol at pH 6.1 and 3.4, respectively, which further indicate that the protein is more easily denatured at acidic pH values. Many published literatures have reported the similar thermal denaturation mechanism of their model proteins such as thermolysin and lysozyme [12,13].

4.2. Protein degradation model for Abbott-X

Several authors have reported that irreversible DSC thermograms could be interpreted in terms of reversible thermodynamics, provided T_m is independent of the heating rate [5,14]. However, we observed that the T_m of Abbott-X varies directly with the heating rate (shown in Fig. 8), implying the presence of an irreversible unfolding transition. In such a transition, the denaturation reaction scheme can be represented by the Lumry–Eyring model (Scheme 1) [15,16].

$$N \underset{k_2}{\overset{k_1}{\rightleftarrows}} U \xrightarrow{k_3} A$$

Scheme 1.

$$N \rightleftharpoons U$$
$$U + U \longrightarrow A^{(2)}$$
$$A^{(2)} + U \longrightarrow A^{(3)}$$
$$\vdots$$
$$A^{(n-1)} + U \longrightarrow A^{(n)}$$
$$A^{(2)} + A^{(2)} \longrightarrow A^{(4)}$$
$$A^{(i)} + A^{(j)} \longrightarrow A^{(i+j)}$$

Scheme 2.

In Scheme 1, N represents the native monomer, U represents the monomer in non-native conformation and A represents the aggregation state. If the rate of aggregation is much faster than that of renaturation ($k_3 \gg k_2$), the non-native molecules will be converted into aggregates instead of returning to the native state. Therefore, the transition of denaturation or unfolding (from N to U) appears as if it follows a first-order process.

4.3. Kinetic analysis of thermal-induced aggregation of Abbott-X

The observed protein aggregation kinetics measured by SEC may be interpreted as first-order, second-order or the combination of first and second-order reactions depending on the specific protein studied [5,15,16]. Roberts et al. developed and described a kinetic model in which a general reaction mechanism for aggregation through the non-native conformation, U, could be given as shown in Scheme 2 [16,17] which can be viewed as an extended version of Lumry–Eyring model described in Scheme 1.

The above aggregation reaction scheme can be mathematically described as the combination of first- and second-order reaction expressed as Eq. (3):

$$\frac{dM}{dt} = -2k_{agg2}M^2 - k_{agg1}M \quad (3)$$

where M stands for monomer unfolded protein, dM/dt is the rate of degradation or rate of monomer loss, k_{agg2} is the apparent rate constant for the irreversible dimerization process and the apparent rate constant k_{agg1} characterizes a subsequent cascade of further aggregation steps. It is a rate law for monomer loss combining first- and second-order processes.

As described above, the aggregation of Abbott-X monoclonal antibody at studied pH values was confirmed by micro-DSC to follow through the non-native conformation route. This suggests that reaction Scheme 2 can be used to determine the kinetic parameters of aggregation for this model protein. The SEC data obtained for Abbott-X at each temperature was fitted by each model of first-order, second-order and the reaction Scheme 2 (Eq. (3)),

$$N \xrightarrow[\Delta H_{un}]{k_{un}} U$$
$$U \xrightarrow[\Delta H_{agg1}]{k_{agg1}} A$$
$$U + U \xrightarrow[\Delta H_{agg2}]{k_{agg2}} A$$

Scheme 3.

Table 2
Rate constants of unfolding and aggregation of monoclonal antibody Abbott-X at pH 3.4 obtained from TAM and SEC.

Temperature (°C)	Estimated k_{un} 1/s (unfolding)	Estimated ΔH_{un} J/g (unfolding)	Estimated k_{agg1} 1/s (aggregation)	Estimated ΔH_{agg1} J/g (aggregation)	Estimated k_{agg2} ml/(g s) (aggregation)	Estimated ΔH_{agg2} J/g (aggregation)	K_{obs1} 1/s (aggregation)	K_{obs2} ml/(g s) (aggregation)
55	3.56E−5	14.7	5.16E−5	−4.27	0.0096	−5.5	4.64E−5	0.0077
58	8.06E−5	24.4	1.24E−4	−5.5	0.0099	−19	1.25E−4	0.0089

k_{un}, k_{agg1}, k_{agg2}, ΔH_{un}, ΔH_{agg1}, ΔH_{agg2} were obtained from power–time curve fitting. k_{obs1} and k_{obs2} were obtained by SE-HPLC data fitting.

respectively. One of the fitted curves, the total monomer concentration at pH 3.4 over time at 55 °C using Eq. (3) is shown in Fig. 4. Statistically, the observed thermally induced aggregation kinetics of Abbott-X can be best described by Scheme 2 (Eq. (3)) after comparison of the model selection criterion[1] for all three fitted models (3.8 for first-order, 5.4 for second-order and 6.8 for the combination of first- and second-order).

4.4. Deconvolution of the thermal signal from isothermal calorimetry

As discussed above, Abbott-X's unfolding can be described as a first-order process, while the subsequent aggregation is a combination of first- and second-order processes. Because of its non-specific nature, the thermal activity monitor (TAM) measures the overall thermal activity of Abbott-X under isothermal conditions. With the knowledge obtained from micro-DSC and SEC, the overall heat flow monitored by TAM could be deconvoluted and simplified as Scheme 3.

In Scheme 3, rate constant k_{un} characterizes the pseudo-first-order of N to U transition with endothermic ΔH_{un}, while rate constants k_{agg1} and k_{agg2} characterize the consequent aggregation processes with exothermic ΔH_{agg1} and ΔH_{agg2}, respectively. Recently, Beezer et al. introduced a method for the determination of the kinetic parameters and reaction enthalpies of a consecutive reaction scheme [18]. This method requires a kinetic equation as a function of heat flow. This can be done if the consecutive reactions are all obeying first-order kinetics as described by the authors. However, for the consecutive reactions involving second-order or more complicated order reactions, it is difficult or even impossible to solve the integrated rate equations. In this study, we used Scientist software, which allows the users to input the differential equations directly instead of solving the complicated integrated equations to calculate the rate constants. The differential calorimetric equations input into the software that describe the reaction Scheme 3 are:

$$\frac{dN}{dt} = -k_{un}N \tag{4}$$

$$\frac{dU}{dt} = k_{un}N - 2k_{agg2}U^2 - k_{agg1}U \tag{5}$$

$$\frac{dA^2}{dt} = 2k_{agg2}U^2 \tag{6}$$

$$\frac{dA^{(n)}}{dt} = k_{agg1}U \tag{7}$$

$$W = -V\left(\Delta H_{un}\frac{dN}{dt} - \Delta H_{agg2}\frac{dA^{(2)}}{dt} - \Delta H_{agg1}\frac{dA^{(n)}}{dt}\right) \tag{8}$$

where W is the power signal (μW) and V is the volume of the sample (mL), N is the native monomer (g/mL), U is the non-native monomer (g/mL), $A^{(2)}$ is the dimer and $A^{(n)}$ represents the aggregates with higher MW ($n = 1$ in this case).

The fitted power–time plot for Abbott-X at pH 3.4 at 55 °C using Eq. (8) is represented in Fig. 5 (black thin line) with the model selection criterion of 6.7, and the fitted rate constants are shown in Table 2. The rate constants calculated by power–time curve fitting (Eq. (8)) are in a good agreement with those obtained from SEC data fitting (Scheme 2), demonstrating that the deconvolution of the power–time curve of thermal-induced protein aggregation is possible using Eq. (8), therefore, this method can quantitatively predict the kinetic parameters.

4.5. Approach to protein formulations screening using isothermal calorimeters

The screening conducted in the calorimeters (DSC and isothermal microcalorimetry) allows rapid assessment of the stability of small molecule pharmaceuticals and active pharmaceutical ingredient (API)-excipient compatibility in formulations [10,19,20]. It is also possible to use a similar approach to determine the optimal pH range of macromolecule formulations by determining protein unfolding and aggregation. The optimal pH range for Abbott-X was found to be between pH 5 and pH 6 by simply comparing T_m and the slope of power–time curves. With knowledge of the reaction kinetics model, a complete thermodynamic and kinetic description of a process in solution can be obtained from power–time curves using isothermal microcalorimetry without further experimentation [18,21]. In combination with the kinetics model for Abbott-X's unfolding and subsequent aggregation determined using SEC and DSC, the aggregation rate constants could be obtained by deconvoluting the power–time curve. Because a large number of proteins follow similar thermal-induced aggregation pathways, the isothermal approach could also be feasible to other protein pharmaceuticals with small modification, if needed. Recently, Beezer et al. described a model free approach which does not require the knowledge of reaction mechanism, to deconvoluting thermal data by using the chemometric analysis [22]. This approach requires at least $2n+2$ repeated experiments to allow possible data analysis (n is the number of reaction processes). Since the methodology was established using small organic molecules as model compounds, it is certainly worth while to explore Beezer's model free approach on proteins in the future.

5. Conclusion

Isothermal microcalorimetry has previously been extensively studied as a tool in monitoring the stability of small molecule pharmaceuticals and determining excipient compatibility in formulation development of small molecules. We have demonstrated that this same technique may be used for the same purpose with application to protein pharmaceuticals. A developmental monoclonal antibody, Abbott-X, was selected as a model protein to test the feasibility of this technique. We found that it is possible to deconvolute the observed power–time (TAM) data of protein degradation so that the detailed kinetic parameters can be obtained directly from TAM data without using labor-intensive SEC to obtain

[1] Model selection criterion (MSC): a modified Akaike Information Criterion (AIC), gives the same rankings between models as the AIC and has been normalized so that it is independent of the scaling of the data points. More detailed information regarding can be found in http://www.micromath.com.

concentration versus time data. In addition, the stability rank order of different protein formulations can be readily predicted by comparing the slopes of power–time curves. The work presented here shows that a rapid TAM-based approach is feasible and has the potential to be applied as a screening method for protein pharmaceutical stability at early development stages.

Acknowledgements

The authors are thankful to the parenteral formulation development group of Abbott Laboratories for providing the Abbott-X.

References

[1] W. Wang, Int. J. Pharm. 185 (1999) 129–188.
[2] L. Runkel, W. Meier, R. Pepinsky, M. Karpusas, A. Whitty, K. Kimball, M. Brickelmaier, C. Muldowney, W. Jones, S. Goelz, Pharm. Res. 15 (1998) 641–649.
[3] R. Bartkowski, R. Kitchel, N. Peckham, L. Margulis, J. Protein Chem. 21 (2002) 137–143.
[4] C. Giancola, S. De, D. Fessas, et al., Int. J. Biol. Macromol. 20 (1997) 193–204.
[5] A.W.P. Vermeer, W. Norde, Biophys. J. 78 (2000) 394–404.
[6] S.R. Tello-solis, A. Hernandez-arana, Biochem. J. 311 (1995) 969–974.
[7] B.S. Kendrick, J.L. Cleland, X. Lam, et al., J. Pharm. Sci. 87 (1998) 1069–1078.
[8] A.E. Beezer, S.G. Andrew, R.J. Willson, et al., Int. J. Pharm. 179 (1999) 159–165.
[9] R.L. Remmele, S.D. Bhat, D.H. Phan, et al., Biochemistry 38 (1999) 5241–5247.
[10] E.A. Schmitt, K. Peck, Y. Sun, et al., Thermochim. Acta 380 (2001) 175–183.
[11] F. Wolfgang, Applications of Biocalorimetry Conference, Heidelberg, Germany, 2008.
[12] J.M. Sanchez-Ruiz, J.L. Lopez-Lacomba, et al., Biochemistry 27 (1988) 1648–1652.
[13] J.M. Sanchez-Ruiz, Biophys. J. 61 (1992) 921–935.
[14] C.Q. Hu, J.M. Sturtevant, Biochemistry 26 (1987) 178–182.
[15] R. Lumry, H. Eyring, J. Phys. Chem. 58 (1954) 110–120.
[16] C.J. Roberts, J. Phys. Chem. 21 (2003) 1194–1207.
[17] C.J. Roberts, J. Pharm. Sci. 92 (2003) 1095–1111.
[18] S. Gaisford, A.K. Hills, A.E. Beezer, et al., Thermochim. Acta 328 (1999) 39–45.
[19] G. Bruni, L. Amici, V. Berbenni, A. Marini, A. Orlandi, J. Therm. Anal. Cal. 68 (2002) 561–573.
[20] P. Mura, G.P. Bettinetti, M.T. Faucci, A. Manderioli, P.L. Parrini, Thermochim. Acta 321 (1998) 59–65.
[21] C.V. Skaria, S. Gaisford, M.A. O'Neill, G. Buckton, A.E. Beezer, Int. J. Pharm. 292 (2005) 127–135.
[22] M. O'Neill, A.E. Beezer, J. Tetteh, S. Gaisford, M. Dhuna, J. Phys. Chem. B 111 (2007) 8145–8149.